Sensing and Bio-Sensing Research xxx (xxxx) 100781

Contents lists available at ScienceDirect

Sensing and Bio-Sensing Research

journal homepage: www.elsevier.com/locate/sbsr

A screen-printed carbon electrode modified with a green synthesized gold nanoparticle for selective detection of nitrite in drinking water sample☆

M.V. Arularasu [a,*], T.V. Rajendran [b], R. Vignesh [c], Vinod Kumar Nelson [d], Shaik Mohammed Yusuf [e,*]

[a] Sustainable Energy and Environment Research Unit, Department of Physiology, Saveetha Medical College, Saveetha Institute of Medical and Technical Science, Chennai 602 105, Tamil Nadu, India
[b] Department of Chemistry, SRM University, Ramapuram Campus, Chennai 600 089, Tamil Nadu, India
[c] Department of Chemistry, Arignar Anna Govermemnt College, Cheyyar 604 407, Tamil Nadu, India
[d] Department of Pharmaceutical Chemistry, Mahathi College of Pharmacy, Madanapalle 517319, Andhra Pradesh, India
[e] College of Health Sciences, Debre Tabor University, PO Box 272, Debre Tabor, Ethiopia

ARTICLE INFO

Keywords:
Gold nanoparticle
Green synthesis
Nitrite senor
Linear sweep voltammetry

ABSTRACT

Nanomaterials are used in numerous applications such as medicine, environmental remediation, food packaging, and biomedical applications. Nanoparticle synthesis using the eco-friendly technique shows a fascinating property compared to conventional chemical route methods. In this work, we demonstrate an eco-friendly synthesis of gold nanoparticles (AuNPs) using the *Acacia nilotica* leaf extract. AuNPs modified screen-printed electrode was applied for electrochemical detection of nitrite. Synthesized AuNPs were characterized by various techniques, including FT-IR, XRD, FE-SEM, TEM, EDX, and UV–visible analysis. FT-IR result of AuNPs demonstrate the distinct functional groups involved in the formation of AuNPs. FE-SEM confirms the AuNPs towards agglomeration and tiny nanoparticles were obtained in uniformly spherical in shape. The TEM analysis revealed AuNPs have small spherical nanoparticles with a size ranging from 10 to 20 nm and EDX result displayed the presence of Au element. The UV–visible absorbance band appeared at 584 nm due to surface plasmon resonance, which confirms the reduction of Au ions to elemental AuNPs. At optimized conditions, a wide linear response range from 0.1 to 1000 μM and a relatively low detection limit (0.03 μM) was observed for electrochemical detection of nitrite ion by modified AuNPs/SPCE electrode. Moreover, the sensor demonstrates outstanding repeatability, selectivity, reproducibility, and storage stability. Thus, the fabricated, AuNPs/SPCE electrode has versatile, practical applications for detecting nitrite in aquatic media.

1. Introduction

Nanoparticles (NPs) have a unique property compare to the bulk counterparts due to their small size and large surface-to-volume ratio, therefore NPs can be used for various applications [1,2]. Metal NPs synthesize using physical, chemical, or electrochemical approaches can be expensive and time-consuming, and there are some limitations on usage, for example using many toxic substances can be used for above method would create negative environmental impact [3]. For the above reason, the green nanotechnology and eco-sustainability approach have gained more attention now-a-days. Utilizing plant materials part such as seeds, flowers, roots, and leaves was proven to be a safer and eco-friendly option for producing metal NPs. Such methods are endowed with numerous phytochemicals like flavonoids, alkaloids, polyphenols, etc., which would help to produce a green reduction of metal ions into the respective NPs via a single-step process, further helping to regulate the size and shape of NPs [4,5]. *Acacia nilotica* is composed of variety of phyto-constituents including ellagic acid, tannins, triterpenoids, flavonoids, isoquercitin, saponins, leucocyanidin which could help to biosynthesis of AuNPs via a single-step reduction process.

Nitrite ion (NO_2^-) is a most common inorganic compound and has been used for food preservation and corrosion inhibitor in our daily life [6,7]. If human body contain excess nitrite levels can accelerate the irreversible oxidation of hemoglobin to methemoglobin (Fe^{2+} is oxidized to Fe^{3+}), which leads to central nervous system, birth defects, spontaneous abortion, and intrauterine growth restriction [8,9]. Because of its potential toxic effects of nitrite, the World Health Organization has reported that the fatal dose of nitrite intake per daily limit should be

☆ This article is part of a Special issue entitled: 'Green synthesis sensors' published in Sensing and Bio-Sensing Research.

* Corresponding authors.
E-mail address: mdyusuf.pharma@dtu.edu.et (S.M. Yusuf).

https://doi.org/10.1016/j.sbsr.2025.100781
Received 14 February 2025; Received in revised form 20 March 2025; Accepted 24 March 2025
2214-1804/

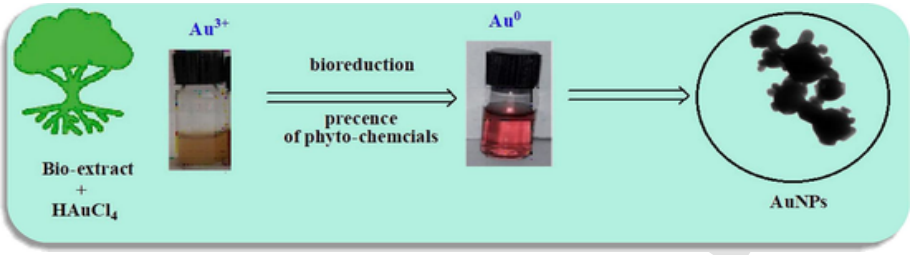

Scheme 1. Photo images of (i) leaf extract and (ii) AuNP extract

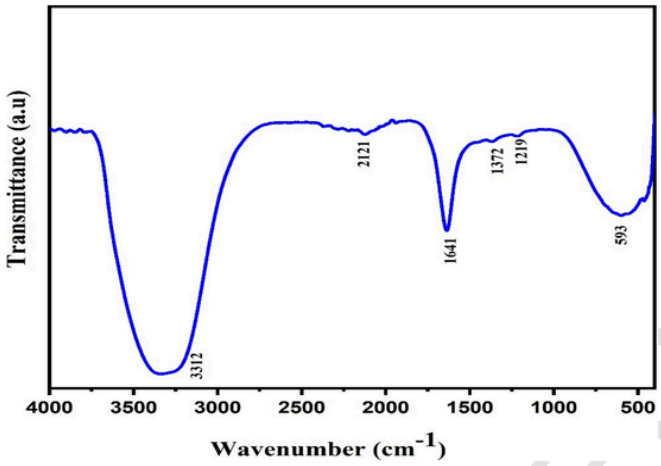

Fig. 1. FT-IR result of AuNPs.

≤0.07 mg/kg for humans. Therefore, is an immense need to develop reliable, rapid, quick methods for the detection and monitoring of nitrite to supervise the quality of water and food sample. Numerous methods have been developed for nitrite detection, including high-performance liquid chromatography, spectrophotometry, colorimetry, chemiluminescence, and electrochemical detection [10–12]. Among them, electrochemical detection possesses powerful tools due to rapidity, simple instrumentation, low cost, and high sensitivity methodologies that have become widespread research interest, which is more favored for the detection of nitrite. Unfortunately, the electrochemical method is still a challenge for sensitivity due to some serious defects, such as the high oxidation potential of nitrite during electrochemical oxidation at traditional electrodes, slow kinetics, and electrode surface contamination. Therefore, various effort has been focused on electrochemical sensors to enhance the sensitivity towards nitrite ion detection. More recently, metal nanoparticles (NPs) have received considerable interest due to the enhancement of high electron transport, high effective surface area, unique dimensions, excellent catalysis, and biocompatibility [13–15].

In this present work, electrochemical nitrite sensing properties using AuNP synthesized from *Acacia nilotica* extract has never been investigated in earlier literature. We used the green synthesized AuNPs for the modification of SPCE electrode and for highly sensitivity sensing of nitrite. The practical and reliability performance in real samples were also performed and showed satisfactory results.

2. Experimental section

2.1. Chemical and reagents

All reagents were used in this work are A.R grade. Chloroauric acid ($HAuCl_4$, 99.9 %), sodium nitrite ($NaNO_2$, 99 %), sodium benzoate (C_6H_5COONa, 99 %), 4-nitrophenol ($C_6H_5NO_3$, 99 %), butylated hydroxytoluene ($((CH_3)_3CC_6H_3(OCH_3)OH$, 98.5 %), calcium hydroxide ($Ca(OH)_2$, 95 %), copper hydroxide ($Cu(OH)_2$, 95 %) were purchased from Merck India Ltd. and used without further purification.

2.2. Preparation of leaf extract

The fresh, healthy leaves of *Acacia nilotica* were obtained in Tiruvallur, Tamil Nadu, India. The leaves of *Acacia nilotica* were washed several times with de-ionized water to clean the dust and dried at room temperature for 7 days to drain out moisture, further grounded to a fine powder. 10 g of the powder was boiled with 100 mL of de-ionized water at 50 °C for 20 min, and the extract was twice filtered using Whatman filter paper, and the collected solution was placed in the refrigerator for further analysis.

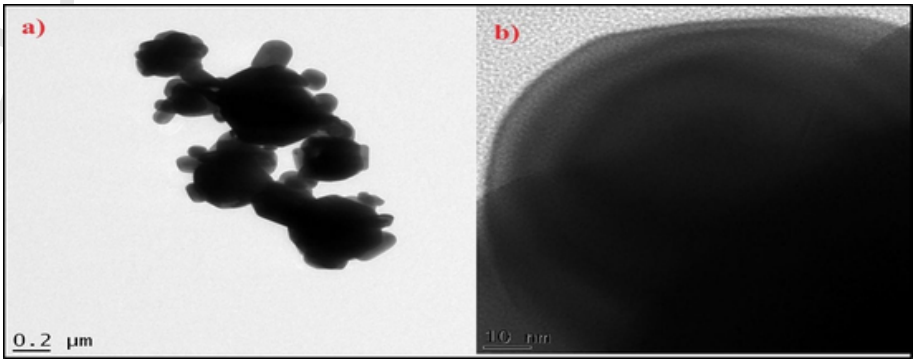

Fig. 2. (a-b) TEM images at different magnifications of AuNPs.

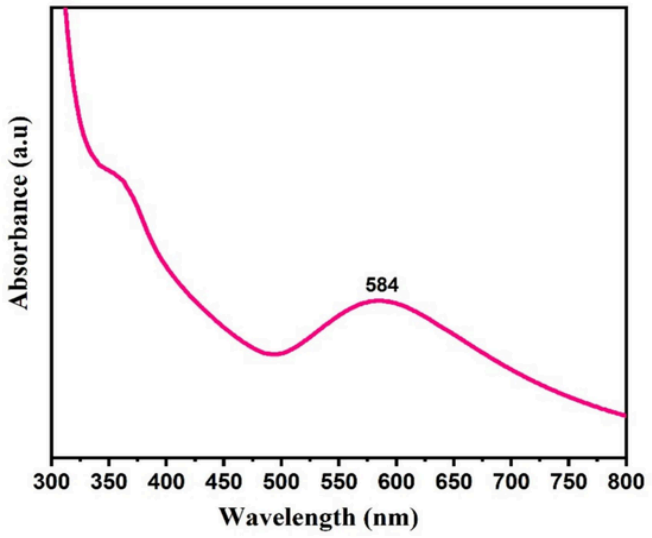

Fig. 3. UV–Visible images of AuNPs.

2.3. Green synthesis of AuNPs

10 mL of *Acacia nilotica* leaf extract was gradually mixed into a 1 mL of 0.0011 M aqueous solution of $HAuCl_4$ under vigorous stirring, after 24 h of stirring a noticeable change in the reaction mixture's color was observed (from light yellow to purple-red) which confirm the formation of AuNPs. This color shift is attributed to the reduction of Au^{3+} ion into AuNPs, a phenomenon associated with surface plasmon resonance (SPR). To validate the process, a control experiment without $HAuCl_4$ was also conducted. Subsequently, the colloidal solution underwent purification through centrifugation at 6000 rpm for 20 min, followed by multiple washes with de-ionized water to remove impurities and by-products. The resulting AuNPs were dried at 60 °C and stored at 27 °C for further characterization. (Scheme 1, illustrating the AuNPs preparation method).

2.4. Characterization

Following the formation of AuNPs, experimental methodologies were employed to assess their functional group composition, surface textures (encompassing both shape and size), elemental composition, crystalline structure, and optical characteristics. Functional group analysis was performed by FT-IR spectroscopy (JASCO FT/IR-6600 spectrometer). Crystalline phase was analyzed using XRD (Shimadzu XRD 6000) with CuKα as the radiation source. The surface morphology was investigated by FE-SEM with EDX (HITACHI S-3000 N) and TEM (Jeol/JEM 2100) analysis. The UV–visible light absorption ability was measured by UV–Vis double beam spectrometer (UV-2450).

3. Preparation of electrode for electrochemical sensor

The disposable SPCE (screen-printed carbon electrode) was cleaned carefully with double distilled water (DD). After that, 5 μL of AuNPs solution was drop-casted onto the SPCE, and then the modified SPCE was allowed to dry for 30 min at 70 °C. Finally, the modified electrode was further investigated for electrochemical measurements by employing a three-electrode system using as-prepared SPCE as a working electrode, Ag/AgCl as a reference electrode, and Pt wire used as a counter electrode.

3.1. FT-IR and XRD analysis

The presence of the functional groups contributing to the reduction and stabilization of AuNPs during synthesize process were analyzed using FT-IR spectroscopy. The typical FT-IR peaks of AuNPs are represented in Fig. 1. The strong absorption peaks appeared at 593 cm^{-1}, 1219 cm^{-1}, 1372 cm^{-1}, 1641 cm^{-1}, 2121 cm^{-1}, and 3312 cm^{-1} in the region of 450 to 4000 cm^{-1}. The peak formed at 3312 cm^{-1} is associated with the N-H/O-H stretching of the phenols and alcohol group [16]. The characteristic bands at 2121 cm^{-1}, 1641 cm^{-1}, 1372 cm^{-1} and 1219 cm^{-1} in AuNPs are assigned to the C—C stretching, =CO bending, C—N stretching, primary or secondary OH in-plane bending respectively [17–20]. The remaining peaks corresponding to medium C—Br stretch bong, which belongs to the alkyl halide groups [21]. The result confirmed that the phytochemical groups present in the extract it could be act as capping, reducing, and stabilizing agents during AuNPs synthesis.

Further, the crystalline nature and phase structure of the synthesized AuNPs were investigated using XRD analysis. From Fig.S1, three major peaks appeared at 38.05°, 44.53°, and 64.31°, corresponding to (111), (200), and (220) Brag reflections (2θ), which confirm the face-centered cubic (fcc) phase of AuNPs (JCPDS file no. 01–1174). Additionally, the average crystalline size of AuNPs was calculated using the Scherrer equation, and the average sizes were around ≈ 20 nm by considering reflection corresponding to the (111) plane. The XRD reflections confirmed a single-phase, and high crystalline nature of synthesized AuNPs.

3.2. Morphology and elemental analysis of AuNPs

The morphological, size, and shape of the AuNPs were analyzed using FE-SEM and TEM analysis. Fig.S2 illustrates the FE-SEM image of AuNPs morphology, it exhibits spherical and cubic-shaped nanoparticles were aggregated grains of AuNPs. The morphology features of the AuNPs, such as the size and shape of nanoparticles, were further examined by TEM analysis. Fig. 2(a-b) shows the typical TEM images of green synthesized AuNPs at two different magnifications. The obtained results revealed that spherical shape was predominant of the NPs. EDX analysis is used to confirm the bio reduction of Au^{3+} into AuNPs through typical signals of elemental Au atom at 2.2, 1.8, 8.5, 9.6, 11.4, 13.5 KeV and it was confirmed that Au (43.76 %), C (16.82 %), O (37.56), Ti (1.95 %) was the significant component in the prepared sample as shown in Fig.S3. Moreover, the EDX spectra also showed other peaks that could originate from the phytochemical of plant extract. The existence of carbon and oxygen elements was responsible for the reduction and stabilization of the AuNPs.

3.3. UV–visible spectroscopy

The optical property of green synthesized AuNPs was analyzed using UV–Visible spectroscopy (Fig. 3). One of the most distinguishing properties of metallic NPs is the surface plasmon resonance (SRP) in UV–Visible spectroscopy. For the AuNPs, a clear and robust SRP peak absorbance at 584 nm, which is confirmed the formation of metallic nanoparticle.

3.4. Electrochemical determination of NO^{2-}

The electrochemical sensing properties of AuNPs/SPCE have been investigated using cyclic voltammetry (CV) measurement. Fig. 4a shows the CVs results of bare SPCE and AuNPs/SPCE in presence of PBS (pH 7.0) containing 100 μM of NO^{2-} (nitrite) at the scan rate of 50 mV s^{-1}. It is obvious that AuNPs/SPCE show greater oxidation peak currents for NO^{2-} than those of bare SPCE. A broad oxidation hump can be observed in the CV results, which was attribute to the strong adsorp-

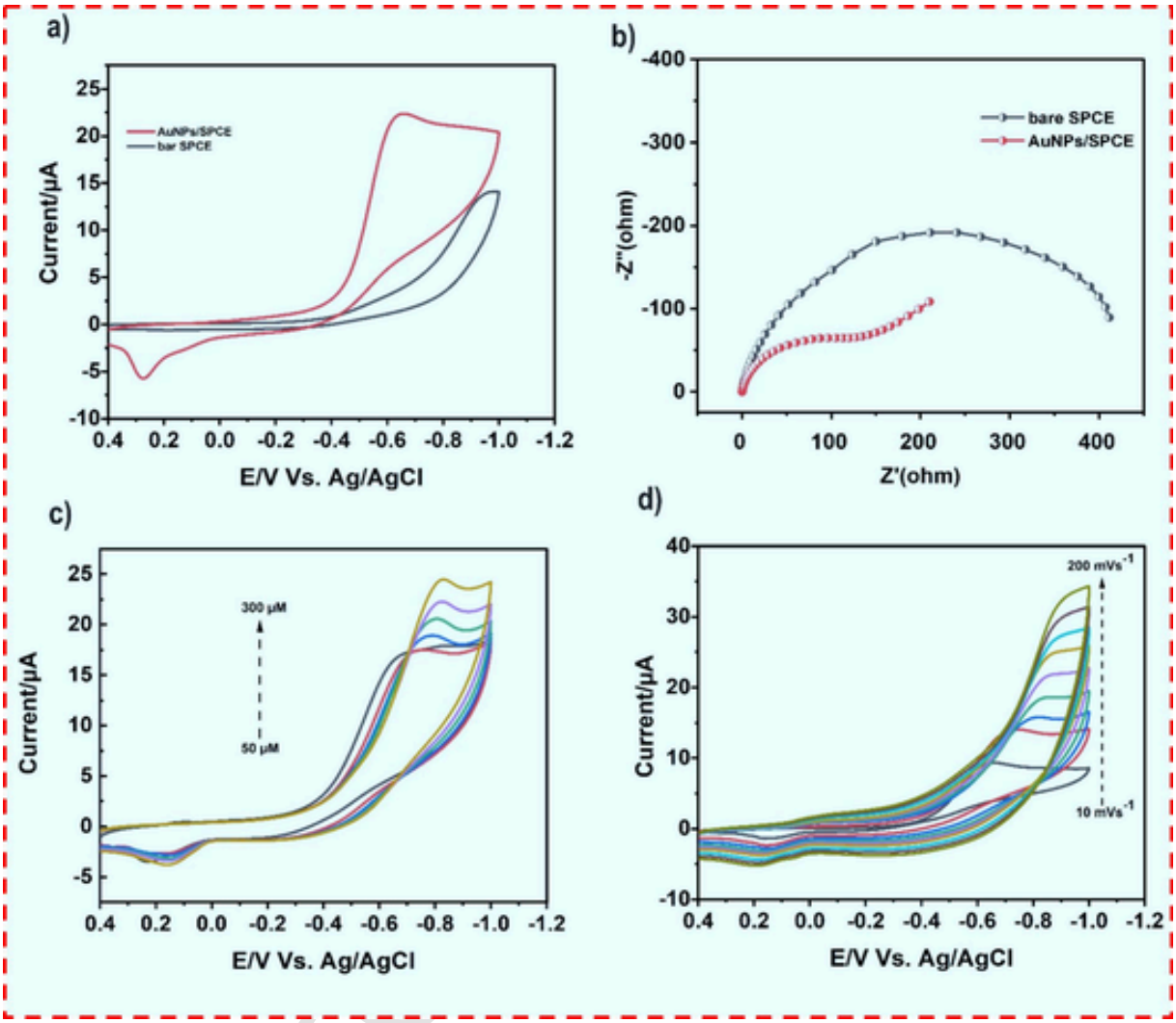

Fig. 4. a) CV plot for the bare SPCE, AuNPs/SPCE in the presence of PBS (pH 7.0) and scan rate of 50 mV s^{-1} with 100 μM concentration of NO^{2-}(nitrite) b) EIS plot of SPCE, AuNPs/SPCE in a 0.1 M KCl solution containing 5 mM of $Fe(CN)_6^{3-/4-}$ with 100 μM concentration of nitrite, c) CV response of AuNPs/SPCE at different concentration of nitrite concentration, d) CV response upon a various scan rate (10–200 mV s^{-1}) at AuNPs/SPCE.

tion and fast electron transfer occurring on the surface of modified electrode. From the results, a peak current gradually shifting towards the positive side of AuNPs/SPCE than bare SPCE, further distinct anodic peak response was observed for AuNPs/SPCE, which suggests slight reduction peak was observed in the reverse scan suggest an irreversible electrochemical reaction. An electrochemical impedance spectroscopy (EIS) investigation was performed to analyze the capacitive behavior and ion-transport performance of the samples. Fig. 4b illustrates the Nyquist plot from EIS of AuNPs/SPCE and bare SPCE electrode materials. As observed in Fig. 4b, the Nyquist plot of bare SPCE showed a semicircle with a larger diameter than the AuNPs/SPCE electrode, representing a large charge transfer resistance (R_{ct}). However, the R_{ct} values of AuNPs/SPCE significantly decrease during electrochemical studies, suggesting the redox reaction occurs successfully at the electrode surface. Obviously, AuNPs/SPCE possess lower R_{ct} at the electrode-electrode interface, indicating that the electrode has better charge transfer ability due to pores on the material, which could shorten the shuttle distance of the ions [22,23].

3.4.1. *Effect of concentration and scan rate*

In this experiment, the performance of AuNPs/SPCE modified electrode with various concentrations of NO^{2-} (50 μM to 300 μM) were measured using CV response. Fig. 4c shows that the anodic current significantly increased with increasing concentration of NO^{2-}. Similarly, the resultant linear response was plotted by different NO^{2-} concentrations and the redox peak current. Fig.S4 illustrates the linear plot of the different concentrations with the regression equation and its correlation coefficient is $y = -0.029\times - 14.806$ and $R^2 = 0.9871$. The obtained result indicates the good electrocatalytic activity of AuNPs/SPCE towards NO^{2-} oxidation.

CV measurements over the AuNPs/SPCE were observed in the presence of NO^{2-} analyte at different scan rates from 10 to 200 mVs^{-1} at pH 7.0 are shown in Fig. 4d. The anodic peak current observed at different sweep rates with increasing the scan rate (10–200 mVs^{-1}), and the linear regression equation is also increased. As illustrated in Fig.S5, that irreversible anodic peak current is proportional to the square root of the scan rate with a correlation coefficient R^2 of 0.9812 and the linear regression equation $y = -0.1190\times - 9.9372$, attained for NO^{2-} analyte from the scan rate analysis. These results clearly support that electrochemical detection of NO^{2-} towards AuNPs/SPCE is a typical diffusion-controlled process.

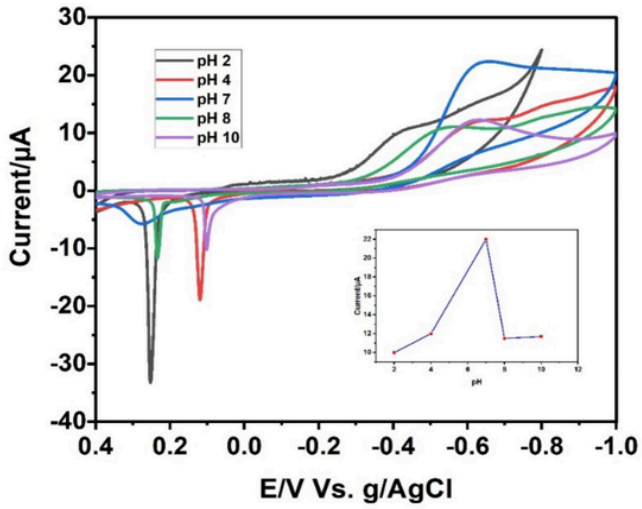

Fig. 5. pH performance of AuNP/SPCE with different pH ranging from 2 to 10.

3.4.2. Effect of pH

The influence of buffer pH on the electrochemical response of AuNPs/SPCE was investigated and the results are shown in Fig. 5. In acidic conditions, owing to the nitrite oxidation, the anodic peak response of nitrite oxidation increased proportionally which also proves that NO^{2-} get easily oxidized to NO^{3-} on the SPCE. Therefore, the pH plays an important role to determine the NO^{2-} analyte. Furthermore, when the pH increases from 3.0 to 7.0, the reduction peak current gradually increases; suddenly, the peak current decreases after pH 7 due to insufficient protons in the increasing basic medium make nitrite oxidation extremely difficult [20]. Therefore, a pH 7.0 solution was chosen for all electrochemical detection studies. On the basis of the previous literature, the possible electrocatalytic oxidation mechanism of nitrite using AuNPs/SPCE in a PBS 7.0 is as follows,

$$Au^0 + NO^{2-} \rightleftharpoons [Au(NO)_2] + e \quad (1)$$

$$[Au(NO)_2] \rightleftharpoons Au^{3+} + NO_2 + e^- \quad (2)$$

$$NO_2 + H_2O \rightleftharpoons 2H^+ + NO_{3-} + NO_{2-} \quad (3)$$

$$Au^{3+} + NO_{2-} + e^- \rightleftharpoons [Au(NO)_2] \quad (4)$$

$$NO_{2-}H_2O + e^- \rightleftharpoons HNO_{2-} + OH^- \quad (5)$$

In the first step, NO^{2-} is adsorbed on the surface of AuNPs/SPCE to form a complex of AuNPs (NO_2^-) are represented in eq. 1, and the complex loses an electron to form NO_2 as depicted in eq. 2. Next, homogeneous disproportionation reaction occurs on NO_2 and form nitrite and nitrate (eq. 2&3). In the reverse scan, the current for the reduction of AuNPs and formation of HNO_2^- as given in eq. 4 & 5.

3.4.3. Electrochemical determination of NO_2^-

The analytical performance of AuNPs/SPCE modified electrode towards NO^{2-} analyte was examined by the linear sweep voltammetry (LSV) technique under the optimized conditions. Fig. 6a,b displays the LSV current response and respective linear regression values of AuNPs/SPCE modified electrode towards various concentrations of nitrite analyte from 0.1 μM to 100 μM and 100 μM to 1000 μM (Fig.S6a&b) with the regression coefficient 0.9784, 0.9823 respectively. Notably, the NO^{2-} analyte electrochemical performance was consistent in a wide concentration range, as confirmed by the linearity of the LSV calibration curve. Moreover, the limit of detection (LOD) was calculated using the following equation;

$$LOD = 3\,S_b/S \quad (6)$$

where S_b signifies the standard deviation of the blank experiment, and S is the slope value. The LOD value was found to be 0.03 μM from the calculation. The NO^{2-} sensing ability LOD was compared with the previously reported sensor and the results represented in Table 1. From the observation the designed AuNPs/SPCE modified electrode indicates an effective electrode for sensing of nitrite in water samples.

3.4.4. Influence of selectivity, repeatability, reproducibility, and stability studies

Detection of a specific analyte is a crucial parameter of an electrochemical sensor due to the many interfering substances that are present in the real samples. Selectivity refers to the sensor's ability to distinguish and respond to a target analyte in the presence of other potentially interfering substances that might be present in the sample matrix. Fiftyfold excess concentrations of a) sodium benzoate, b) 4-nitrophenol, c) butylated hydroxytoluene, d) Cu^{2+} d) Ca^{2+} were used as interference in presence of NO^{2-} using AuNPs/SPCE. However, a fiftyfold concentration of interference along with NO^{2-} analyte did not interfere in the electrochemical detection (Fig. 6(c)).

Repeatability, reproducibility, and stability of the AuNPs/SPCE electrode were examined using LSV in presence of 100 μM of NO^{2-} containing PBS (pH.7.0) buffer. The repeatability of the AuNPs/SPCE electrode was performed and measured in 50 consecutive cycles. The relative standard deviation (%RSD) was obtained with a very low value of 2.6 %, indicating good repeatability (Fig. 6d). Furthermore, the stability was examined its current response after two weeks and the calculated RSD value of 3.6 %, thus indicates the developed sensor has acceptable storage stability (Fig. 7). All results suggest that the AuNPs/SPCE modified electrode exhibits an excellent anti-interference ability, excellent stability, reproducibility and repeatability towards the detection of NO^{2-} analyte due to high active surface area, thus allowing irreversible electron transfer during electrochemical detection, which indicated that the AuNPs/SPCE is suitable for the analytical application.

3.4.5. Real sample analysis

To estimate the feasibility of AuNPs/SPCE modified electrode based NO^{2-} sensors, two real water samples (tap water and drinking water) were collected for practical application by applying the standard addition method. The LSV technique is amplified to determine the unknown concentration of the NO^{2-} in real samples. The LSV responses using the real samples spiked three different NO^{2-} concentrations, which were recorded under the same experimental conditions to confirm the practicability. The recovery results are listed in Table 2; the obtained recovery results were between 97.5 % and 96.3 % which representing good precision and accuracy.

4. Conclusions

In this current study AuNPs was successfully synthesized AuNPs using *Acacia nilotica* extract were spherical, stabilized, capping and reducing agents. Biosynthesized AuNPs morphology and other physical features were characterized using UV–Vis, FE-SEM, TEM, FT-IR, and XRD analysis. A strong SPR band appeared at 584 nm, confirming the formation of AuNPs. From the FE-SEM and TEM analysis, AuNPs were spherical in nature with 10–20 nm in size range. Further XRD analysis confirms that the AuNPs exist in the *fcc* crystal structure. AuNPs/SPCE modified electrode exhibits a wider linear range (0.1 μM to 1000 μM) and a lower detection limit (0.03 μM) and distinguished sensitivity in the presence of common interfering agents towards NO^{2-} detection. Additionally, the AuNPs/SPCE electrode demonstrated excellent repeatability, reproducibility and good stability, making it a great promising candidate for nitrite detection. Importantly, proposed electrochemical sensor's outstanding properties make it viable to detect nitrite in tap

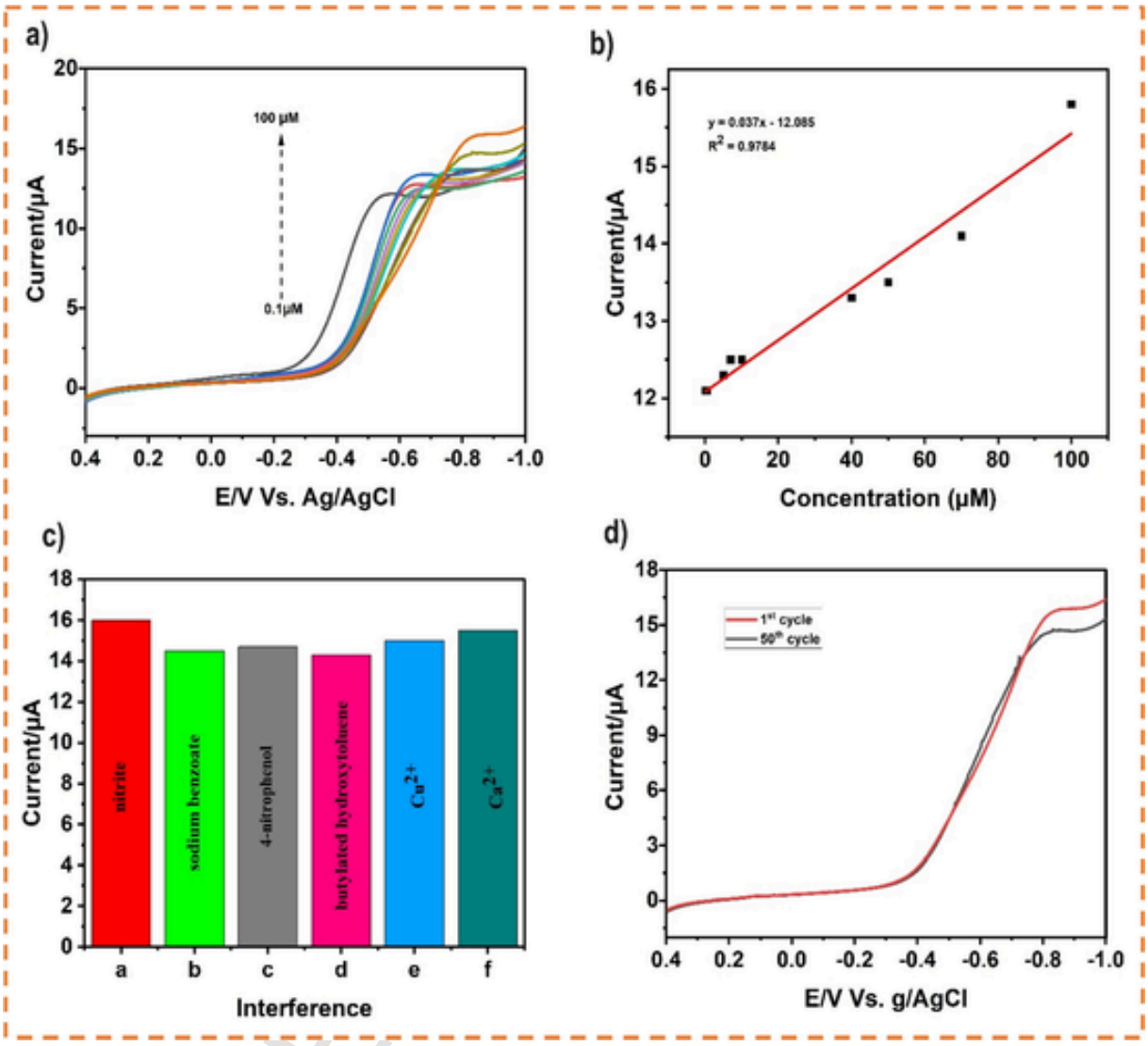

Fig. 6. a) LSV obtained for AuNPs/SPCE having concentration of nitrite from 0.1 to 100 μM, b) plot of nitrite concentration (0.1 to 100 μM) vs anodic peak current obtained for AuNPs/SPCE, c) bar diagram of LSV response of the peak current vs different interference at AuNPs/SPCE d) plot of stability for repeated cycling of AuNPs/SPCE against the cyclic number (1–50 cycles).

water which can get good recovery. Overall, AuNPs could be a good material for sensitive detection of NO^{2-} in aquatic media.

CRediT authorship contribution statement

M.V. Arularasu: Writing – review & editing, Writing – original draft, Validation, Software, Project administration, Methodology, Investigation, Formal analysis, Conceptualization. **T.V. Rajendran:** Writing – original draft, Validation, Software, Resources, Methodology, Investigation, Formal analysis, Data curation. **R. Vignesh:** Writing – original draft, Software, Methodology, Investigation, Formal analysis, Data curation. **Vinoth Kumar Nelson:** Visualization, Validation, Software, Project administration, Methodology, Investigation, Funding acquisition, Formal analysis, Data curation. **Shaik Mohammad Yusuf:** Writing – review & editing, Visualization, Supervision, Resources, Project administration, Funding acquisition, Data curation.

Uncited references

[24–30]

Declaration of competing interest

This paper's authors declare that they do not have any competing financial interests or personal relationships that could influence the findings.

Data availability

Data will be made available on request.

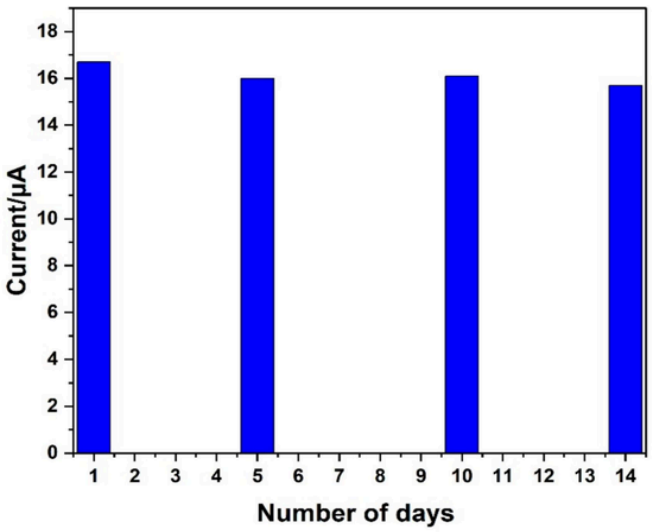

Fig. 7. Histogram representing stability studies of AuNPs/SPCE for 14 days in presence of 100 μM nitrite at 50 mV s^{-1}.

Table 1
Comparison of some characteristics of different electrochemical sensors for the detection of nitrite.

Type of materials	Limit of detection (μM)	Linear range	Method	Reference
AuNPs	0.03	1–100 μM	SWV	24
AuNPs-S-Gr	0.03	12–680 μM	Amperometry	25
AuNP/MoS_2	1.7	0.05–27 mM	Ampe	26
BC/Au/FTO	0.14	0.5 μM-6 mM	DPV	27
LIG/f-MWCNT-AuNPs	0.9	10–140 μM	DPV	28
AuNPs	80 (nm)	0.1 μM –3.8 mM	DPV	8
MWCNTS/AuNPs/ poly melamine	1.14	0.4 μM-1475 μM	DPV	29
Y/Fe modified MWCNT	0.027 (M)	1–1.66 M	LSV	30
AuNPs	0.03	0.1 μM – 1000 0.1 μM	LSV	Present work

FTO- fluorine-doped tin oxide; f-MWCNTS- functionalized multiwalled carbon nanotubes; LIG- laser-induced graphene; BC- biochar.

Table 2
Nitrite determination in real samples using a modified AuNPs/SPCE electrode.

Sample	Spiked (μM)	Found (μM)	Recovery range (%)	RSD (%) $n = 3$
Tap water	0	0	–	–
	5	4.82	97.12	3.21
	10	9.78	97.29	3.18
River water	0	0	–	–
	5	4.72	98.20	3.15
	10	9.59	98.54	3.24

Appendix A. Supplementary data

Supplementary data to this article can be found online at https://doi.org/10.1016/j.sbsr.2025.100781.

References

[1] K. Jyoti, M. Baunthiyal, A. Singh, Characterization of silver nanoparticles synthesized using Urtica dioica Linn. Leaves and their synergistic effects with antibiotics, J. Radiat. Res. Appl. Sci. 9 (3) (2016) 217–227.
[2] T.M. Abdelghany, Recent advances in green synthesis of silver nanoparticles and their applications: about future directions, a review, Bionanoscience 8 (1) (2018) 5–16.
[3] R.A. Hamouda, M.H. Hussein, R.A. Abo-elmagd, S.S. Bawazir, Synthesis and biological characterization of silver nanoparticles derived from the cyanobacterium *Oscillatoria limnetica*, Sci. Rep. 9 (1) (2019) 1–17.
[4] R. Mohammadinejad, S. Karimi, S. Iravani, R.S. Varma, Plant derived nanostructures: types and applications, Green Chem. 18 (2016) 20–52.
[5] A.M. Abdelfatah, M. Fawzy, A.S. Eltaweil, M.E. El-Khouly, Green synthesis of nano-zero-valent iron using ricinus communis seeds extract: characterization and application in the treatment of methylene blue-polluted water, ACS Omega 6 (2021) 25397.
[6] J. Gajdár, S. Rodrigues Gaspar, M. Gabriela Almeida, Trends in nitrite detection: recent advances in electrochemical sensor technologies, TrAC Trends Anal. Chem. 183 (2025) 118105.
[7] S. Anuthum, S. Wiratchan, N. Semakul, J. Jakmunee, K., Ounnunkad signaling redox probe/DNA aptamer complexes on a new POP/2D WSe_2 composite-based immunosensor towards the simultaneous detection of three-protein overexpression as an alternative severe SARS-COV-2 infection diagnosis, Sensors Actuators B Chem. 404 (2024) 135196.
[8] H. Chen, T. Yang, F. Liu, W. Li, Electrodeposition of gold nanoparticles on cu-based metal-organic framework for the electrochemical detection of nitrite, Sensors Actuators B 286 (2019) 401–407.
[9] C. Zou, B. Yang, D. Bin, J. Wang, S. Li, P. Yang, C. Wang, Y. Shiraishi, Y. Du, Electrochemical synthesis of gold nanoparticles decorated flower-like graphene for high sensitivity detection of nitrite, J. Colloid Interface Sci. 488 (2017) 135–141.
[10] T. Pin-Yi Chen, U. Keerthi Reddy, Asma A. Rajaji, M. Govindasamy Alothman, Optimization of electrochemical sensitivity in anticancer drug quantification through ZnS@CNS nanosheets: synthesis via accelerated sonochemical methodology, Ultrason. Sonochem. 105 (2024) 106858.
[11] N. Pardhi, W. Chun Cheng, S.C. Chen, S. Akshay Joshi, M. Govindasamy, A novel strategy towards the fabrication of highly stable and sensitive non-enzymatic glucose sensor based on Ni_3N thin films using high power impulse magnetron sputtering, Appl. Surf. Sci. 669 (2024) 160462.
[12] Arularasu M. Visagamani, M. Harb, K. Kaviyarasu, A. Muthukrishnaraj, M. Ayyar, K.A. Alzahrani, R.H. Althomali, S. Abdulrahman Althobaiti, Electrochemical detection of 4-nitrophenol using a novel $SrTiO_3$/ag/rGO composite, ACS Omega 8 (45) (2023) 42479–42491.
[13] K. Białas, D. Moschou, F. Marken, Electrochemical sensors based on metal nanoparticles with biocatalytic activity, Microchim. Acta 189 (2022) 172.
[14] L. Qian, S. Durairaj, S. Prins, A. Chen, Nanomaterial-based electrochemical sensors and biosensors for the detection of pharmaceutical compounds, Biosens. Bioelectron. 175 (2021) 112836.
[15] F. Mollarasouli, E. Zor, G. Ozcelikay, S.A. Ozkan, Magnetic nanoparticles in developing electrochemical sensors for pharmaceutical and biomedical applications, Talanta 226 (2021) 112108.
[16] E. Urnukhsaikhan, B.E. Bold, A. Gunbileg, N. Sukhbaatar, T. Mishig-Ochir, Antibacterial activity and characteristics of silver nanoparticles biosynthesized from *Carduus crispus*, Sci. Rep. 11 (2021) 21047.
[17] W. Shen, Y. Qu, X. Pei, S. Li, S. You, J. Wang, Z. Zhang, J. Zhou, Catalytic reduction of 4-nitrophenol using gold nanoparticles biosynthesized by cell free extracts of Aspergillus WL-Au, J. Hazard. Mater. 321 (2017) 299.
[18] F. Montero-Silva, N. Duran, M. Seeger, Synthesis of extracellular gold nanoparticles using *Cupriavidus metallidurans* CH34 cells, IET Nanobiotechnol. 12 (2018) 40.
[19] M. Hamelian, K. Varmira, H. Veisi, Green synthesis and characterizations of gold nanoparticles using thyme and survey cytotoxic effect, antibacterial and antioxidant potential, J. Photochem. Photobiol. B 184 (2018) 71–79.
[20] N. Thangamani, N. Bhuvaneshwari, Green synthesis of gold nanoparticles using Simarouba glauca leaf extract and their biological activity of micro-organism, Chem. Phys. Lett. 732 (2019) 136587.
[21] M. Narayanan, S. Divya, D. Natarajan, S. Senthil-Nathan, S. Kandasamy, A. Chinnathambi, T. Awad Alahmadi, A. Pugazhendhi, Green synthesis of silver nanoparticles from aqueous extract of Ctenolepis garcini L. and assess their possible biological applications, Process Biochem. 107 (2021) 91–99.
[22] M.V. Arularasu, J. Devakumar, R. Sundaram, Impedance spectroscopy, magnetic and optical analysis of cadmium tungstate nanoparticles from influence of capping agent additives, J. Supercond. Nov. Magn. 31 (2018) 2983–2990.
[23] M.V. Arularasu, B. Venkatadri, A. Muthukrishnaraj, T.V. Rajendran, K. Kaviyarasu Kezhen Qi, H_2O_2 scavenging and biocompatibility assessment of biosynthesized cellulose/Fe_3O_4 nanocomposite showed superior antioxidant properties with increasing concentration, J. Mol. Struct. 1289 (2023) 135838.
[24] A. Adiraju, R. Munjal, C. Viehweger, A. Al-Hamry, A. Brahem, J. Hussain, A. Kommisetty, C. Jalasutram, O. Kanoun Tegenkamp, Towards embedded electrochemical sensors for on-site nitrite detection by gold nanoparticles modified screen printed carbon electrodes, Sensors 23 (2023) 2961.
[25] S. Ahmad Bhat, S. Ahmad Pandit, Mudasir Ahmad Rather, Ghulam Mohd Rather, Nusrat Rashid, Pravin P. Ingoleb, Mohsin Ahmad Bhat, Self-assembled AuNPs on Sulphur-doped graphene: a dual and highly efficient electrochemical sensor for nitrite (NO_2^-) and nitric oxide (NO), New J. Chem. 41 (2017) 8347–8358.
[26] S. Zhanga, Y. Tanga, Y. Chena, J. Zheng, Synthesis of gold nanoparticles coated on flower-like MoS2 microsphere and their application for electrochemical nitrite sensing, J. Electroanal. Chem. 839 (2019) 195–2.
[27] X. Zhang, R. Sun, Construction of an electrochemical sensor for detection of nitrite by gold nanoparticles immobilized on biochar, Int. J. Electrochem. Sci. 18 (2023) 100219.

[28] S. Nasraoui, A. Al-Hamry, P.R. Teixeira, S. Ameur, L.G. Paterno, M. Ben Ali, O. Kanoun, Electrochemical sensor for nitrite detection in water samples using flexible laser-induced graphene electrodes functionalized by CNT decorated by au nanoparticles, J. Electroanal. Chem. 880 (2021) 114893.
[29] E. Han, L. Li, T. Gao, Y. Pan, J. Cai, Nitrite determination in food using electrochemical sensor based on self-assembled MWCNTs/AuNPs/poly-melamine nanocomposite, Food Chem. 437 (2024) 137773.
[30] U. Shahzad, H.M. Marwani, M. Fazle Rabbee, S.Y. Alfaifi, K.A. Alzahrani, M. Mizanur Rahman Khan, M.M. Rahman, Efficient sensitive detection of nitrite with binary Y/Fe-modified multiwalled carbon nanotube nanocomposite by electrochemical approaches, Mater. Chem. Phys. 328 (2024) 130000.